RJC

RASĀYAN *J. Chem.*
Vol. 16 | No. 1 |85-103| January - March | 2023
ISSN: 0974-1496 | e-ISSN: 0976-0083 | CODEN: RJCABP
http://www.rasayanjournal.com
http://www.rasayanjournal.co.in

SYMMETRICAL SYNTHESIS AND CHARACTERIZATION OF FIVE-COORDINATE In(III) PORPHYRINS WITH SALICYLIC ACID DERIVATIVES

D. Sharma[1], D. Gupta[2], S. Kundan[1,✉], G. D.Bajju[2] and S.Ravichandran[3]
[1]Department of Chemistry and Chemical Sciences, Central University of Jammu, Rahya-Suchani-181143, (J&K), India.
[2]PG Department of Chemistry, University of Jammu, Baba Saheb Ambedkar Road, Jammu Tawi-180016, (J&K), India.
[3]Department of Chemistry, Lovely Professional University, Phagwara–144 411, Punjab, India.
✉Corresponding Author: sujatakundancuj@gmail.com

ABSTRACT

Investigations of the In(III)porphyrin complexes with substituted salicylates(X) as axial ligands have been carried out using electronic and biological studies. Electronic spectra of the complexes are accompanied by shifting of wavelength towards hypsochromic/blue-shift or bathochromic/red-shift along with '*f*' values decided by the nature of the functional groups attached to the salicylate ligand. IR frequencies appear at 550cm^{-1}–400cm^{-1} for In–N(Por) and at 650cm^{-1}–700cm^{-1} for In–O_{SA}. ^{1}HNMR spectra reveal the merging of the salicylate ring with that of the protons of the macrocyclic ring. The ^{13}CNMR studies confirm the resonance of the *meso*-carbon tetraphenyl porphyrin ring between 130ppm to 160ppm and the salicylate ring carbons in the region of 110ppm to 165ppm. Thermal analysis confirms the presence of indium nitride (In-N) in an argon atmosphere from 0ºC to 900ºC. Cyclic voltammetry(CV) revealed the reduced or oxidized properties of these complexes lead to the generation of π-anion or cation radicals by two one-electron transfer reactions. In(III)porphyrin complexes with substituted salicylates were also screened for *in-vitro* antifungal activity(%inhibition) against the microbe *"Acremonium fusidoides spp."* using the PDA method, which shows that the percentage inhibition is inverse to the diameter of the colony. The free-radical scavenging or antiradical activity (%RSA) by the DPPH method reveals that these complexes were absorbance and concentration-dependent.

Keywords: Substituted Salicylates, In(III), Axial Ligation, CV, TG/DTA, %Inhibition, %RSA.
RASĀYAN*J. Chem.*, Vol. 16, No.1, 2023

INTRODUCTION

The *meso*-substituted symmetrical porphyrins derivatives with conjugated systems find application in photodynamic therapy, as particular catalysts, in molecular electronic devices, in non-linear optical (NLO), and in various materials chemistry applications.[1-18]Different porphyrins have been synthesized using peripheral modification and substitution with different metal ions at the core of the porphyrin.[19-23]In this avenue, heavy metal porphyrins like indium(III)porphyrins develop an enhanced optical limiting response, as in the case of, polymethylmethacrylate indium(III)porphyrin (InPor-MMA) shows good optical limiting properties like refraction with reasonable position and reversible saturable absorption both in picoseconds and nanosecond timescale.[24-26]The use of auxiliary ligands coordination to metalloporphyrins is an attractive approach for the synthesis of multi-porphyrin arrays due to the preferred coordination number, geometry, and ligand preference of the metalloporphyrins that allows one to rationally construct these molecules with well-defined geometries.[27, 28]In another example of axially ligated substituted [In-tPP], the non-linear optical properties affected by the axial ligands mainly led to the change in their excited-state absorption cross-section. Herein, we have used salicylic acid (SA) derivatives as axial ligands because they form strong complexes with the salicylate ligands containing phenolates and carboxylate groups.[29]Coordination of phenol in salicylate type complexes is also well characterized by metal(III) ions in the aqueous medium, which can be ascribed to the initial condition of the anionic carboxylate oxygen which serves to anchor the ligand while the phenolate moiety coordinates the secondarily.[25,30]There has been an increasing enormous interest in the biochemistry of metal-salicylate

http://doi.org/10.31788/RJC.2023.1617019

complexes, due to their relevance in the treatment of diverse gastrointestinal disorders as well as in various other fields such as the synthesis of oxide materials from heterometallic precursors, etc.[31-33]Moreover, the substitute salicylates have proven to be versatile ligands that display a wide range of coordination modes that offer ligand geometry with hard and strong basic donor centres, facilitating the chelation by bridging metal cation from a medium- to large-size that should be susceptible to fill its coordination sphere totally.[34-38]Besides, these, the intra-and/or intermolecular hydrogen bonding due to the hydroxyl group in salicylate ions can also engage that assist a multidimensional assembly of the components. With this and many more from the literature, we are eager to see the change in the electronic behavior around In(III)porphyrins, once it coordinates with salicylic acid derivatives.

EXPERIMENTAL

The synthesis of In(III)porphyrins with substituted salicylic acids as axial ligands were prepared by using AR grades chemicals. Pyrrole and propionic acid (Qualigens, India), silica gel (80–120mesh), p-methoxy benzaldehyde (Aldrich, USA), and silica gel (TLC grade, 75μ, Merck, Germany), basic aluminum oxide(Fluka, Switzerland), and $InCl_3$salt was also purchased from Sigma Aldrich. The nitrogen gas was used to degas the entire organic solvents used for the synthesis and dried them before their use. AR grade salicylic acids derivatives (Sisco Research Laboratories Pvt. Ltd.) were used as received.

5,10,15,20-tetrakis(*p*-methoxyphenyl)porphyrin [H_2-tMP]

[H_2-tMP] was synthesized using modified Adler's method (Scheme-I,a) with pyrrole (20mmols) and para-methoxy benzaldehyde20mmols) in propionic acid (50ml) was permitted to reflux at 60°C for half an hour.[39]After the stipulated reaction time, the product was admitted to cool at room temperature for 2hrs. The shiny purple-colored [H_2-tMP] complex was filtered, air-dried, and purified by basic alumina oxide as adsorbent and methanol as the eluting solvent on the glass column. The purified complex finally went for evaporation in the polar solvents and crystallise as a purple solid (60% yield). UV-Vis (nm, CH_2Cl_2): 421 (B-band), 518, 555, 594, 649 (Q-bands); ^{1}HNMR ($CDCl_3$, ppm): -2.10 (s, $2H_{NH}$), 3.95 (s, $12H_{OCH3}$), 7.23 (d, $8H_{ArHm}$), 8.07 (d, $8H_{ArHo}$), 8.79 (s, $8H_{\beta H}$); IR (KBr, ν, cm^{-1}): N-$H_{pyrrole}$ = 3449.87, C-H_{ph} = 2965.12, C-$H_{pyrrole}$ = 800.04, C-N = 1341.22, C=N = 1692.52, C-H_{OCH3} = 2913.08, C-O-C_{sym} = 1010.33, C-O-C_{asym} = 1264.21.

Chloro-In(III)-5,10,15,20-tetrakis(*p*-methoxyphenyl)porphyrin [Cl-In-tMP]

The In^{3+} derivatives of [H_2-tMP] were synthesized according to the Bhatti *et al.* methods with modification (Scheme-I.b).[40] 246mg (0.4mmols) [H_2-tMP] and $InCl_3$, 221mg (1.0mmols) were mixed with glacial acetic acid(30mL) and sodium acetate (0.554g) in 250ml round bottom flask was refluxed for 4hrs at 60°C and was monitored spectrophotometrically from time to time to see the variation in the B- and Q-bands intensities respectively. After some time, the reaction was permitted to cool in the ice bath which persuades the crystallization of the complex so formed. The crystallized product was chromatographed using CH_2Cl_2 as an eluent and re-crystallized from hexane and dichloromethane in a 1:2 ratio(40% yield). UV-Vis (nm, CH_2Cl_2): 424(B-band), 562, 600(Q-bands); ^{1}HNMR ($CDCl_3$, ppm): 3.70 (s, $12H_{OCH3}$), 7.40 (d, $8H_{ArHm}$), 8.62 (d, $8H_{ArHo}$), 9.05 (d, $8H_{ArHo}$), 9.12 (s., $8H_{\beta H}$); IR (KBr, cm^{-1}): C-$H_{pyrrole}$ = 806.28, C-N = 1392.67, C=N = 1616.60, C-H_{Ph} = 2967.47, C-H_{OCH3} = 2911.78, C-O-C_{sym} = 1011.24, C-O-C_{asym} = 1298.22.

Conversion of Chloro-In(III)-5,10,15,20-tetrakis(*p*-methoxyphenyl)porphyrin to Hydroxy-In(III)-5,10,15,20-tetrakis(*p*-methoxyphenyl)porphyrin[OH-In-tMP]

A solution of [Cl-In-tMP] was prepared in dichloromethane and washed three times with 2*N* KOH and water respectively. After the extraction, the extracted phase was dried over anhydrous Na_2SO_4 to yield [OH-In-tMP] which was then crystallized from hexane and dried under vacuum.

In(III)-5,10,15,20-tetrakis(*p*-methoxyphenyl)porphyrin with Axial Ligands [X-In-tMP] [X= Salicylic acids derivatives]

To a solution of [OH-In-tMP] (0.03mmol) in 10ml $CHCl_3$, substituted salicylic acid(SA) (15mmol) was mixed and stirred for 12hrs at room temperature. After the stipulated time period, the solution mixture

was evaporated forming varying colours of axially ligated In(III)porphyrin derivatives (20-25% yield)(scheme-I,c).

Detection Method

Shimadzu spectrophotometer was used for monitoring the FTIR of the complexes using KBr pellets. Bruker spectrometer, model AV 400 N (400 MHZ), was used for recording the ^{1}HNMR spectral studies in deuterated chloroform and tetramethylsilane. PG (T-90) spectrophotometer was used for the determination of UV-Visible spectral studies with $CHCl_3$, CH_2Cl_2, and CH_3COCH_3 as solvents. The excitation spectrum was studied on Synergy MX Biotek Multimode reader at ambient temperature. Elemental analysis (C,H,N,S) was analyzed microanalytically on Elemental Analyzer elementary Vario EL III, at 1000ºC using carrier gas like helium and oxygen for combustion. The Finnigan 3300 instrument was used for monitoring the mass spectra using chloroform or methanol as solvent. Cyclic voltammetry (CV) measurements were carried out in 10^{-3}M CH_2Cl_2 solution using KNO_3 solution as supporting electrolyte using BAS CV 50W electrochemical analyzer. The TGA/DTA was performed using Linseis STA PT-1000ºC at a heating rate of 10ºC/min.

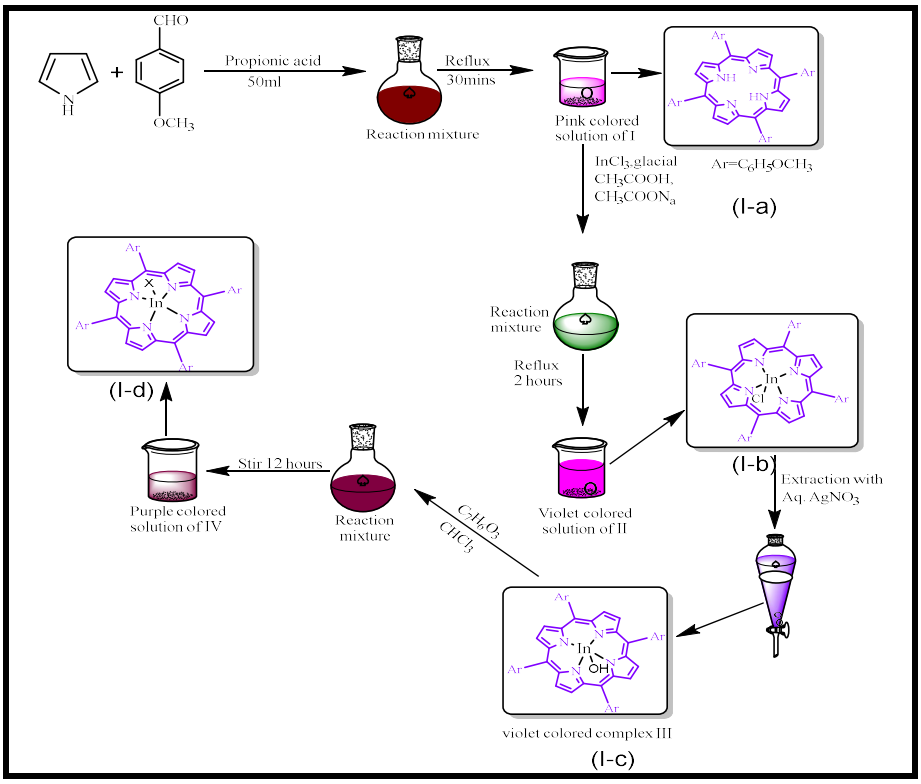

Scheme-I: Proposed Scheme in the Reaction Synthesis of In(III)porphyrin Complexes with Salicylic Acid Derivatives

RESULTS AND DISCUSSION

UV-Visible/Electron Absorption Spectroscopy

The different axially ligated In(III)porphyrins derivatives (Table-1) possess one Band two Q-bands at a different wavelength and absorption coefficient(ε) respectively. The study of absorption data of [X-In-t(*p*-OCH_3)$_4$PP] (X = substituted salicylic acids as an axial ligand) shows a slightly longer wavelength or bathochromic shift(red-shift) for electron-donating substituent whereas shift to shorter wavelength is observed for electron-withdrawing substituents. The more pronounced bathochromic shift occurs in [4-ASA-In-t(*p*-OCH_3)$_4$PP] and [5-ASA-In-t(*p*-OCH_3)$_4$PP] whereas other substituted salicylic acids show minor shifts. Further, the electronic spectra of [X-In-t(*p*-OCH_3)$_4$PP] show a minor variation in the values of λ_{max} and absorption coefficient(ε) but there is a remarkable enhancement in 'Fwhm'($v_{1/2}$) and oscillator strength '*f*' values that increase with the increase in the polarity of the solvent. The $\pi \rightarrow \pi^*$ transitions

undergo bathochromic shifts (red-shifts) with the increase in the polarity of solvents like acetone(CH_3OCH_3), dichloromethane(CH_2Cl_2), and chloroform($CHCl_3$) in the order: CH_3OCH_3>CH_2Cl_2>$CHCl_3$ because in polar solvents the ground state is not more polar than excited state whereas, in the less polar solvents, there observed drift in the spectral band for a less period of time for the axially ligated In(III)porphyrin complexes. For the complex [4-ASA-In-t(*p*-OCH_3)$_4$PP] (Fig.-1), λ_{max} values in acetone were observed at 441nm, 564nm, 606nm while in dichloromethane and chloroform, values were observed at 440nm, 563nm, 604nm, and 437nm, 560nm, 603nm respectively. The '*f*' values for B- and Q-bands were observed at 1.363, 0.622, 0.313 in acetone, 1.344, 0.527, 0.252 in dichloromethane and 1.090, 0.545, 0.252 in chloroform respectively, show a little variation in the oscillator strength(*f*) value. It was also explored that among the different substituted axially ligated In(III)porphyrins, there is a continuous widening of the B- and Q- bands with the enhancement in the polarity of the solvents, which results in the change of '*f*' values and the comparative strength of $\pi\rightarrow\pi^*$ interaction. Thus, it can be concluded that the UV-Vis spectra for precursor porphyrin and axially ligated In(III)porphyrins with B-band centered around 418nm and for Q-bands are red/blue shifted due to the different substituted salicylic acids. These spectral changes are observed by the effects of the substituents on the electron densities of the porphyrin ring and the same basis was accounted for axially ligated indium(III)porphyrin derivatives. Moreover, the red-shifting of B- and Q-bands for complexes containing electron-releasing groups (like $–NH_2$) can be attributed to the lowering of the energy gap between the ground and excited state of the metalloporphyrin moiety whereas the blue shift of bands was observed in the electron attracting groups (like –Cl, -F, $-SO_3H$, $-NO_2$) can be attributed due to the difference in energy gap between the HOMO-LUMO of In(III)porphyrin complexes.

Infra-Red Spectroscopy

The presence of In-O_{SA} bond in various salicylates of In(III)porphyrins complexes through axial coordination was confirmed by the appearance of frequency bands between 600cm^{-1}-650cm^{-1} respectively. The IR spectra of [H_2-t(*p*-OCH_3)$_4$PP] show characteristic IR vibrations of their respective functional groups in which -NH vibrates at 3449.87cm^{-1}, aromatic -CH at 2965.12cm^{-1}, -CN at 1341.22cm^{-1}, -C=C at 1594.22cm^{-1}, -C=N at 1629.52cm^{-1} and $–CH_{OCH3}$ vibrates at 2913.08cm^{-1}, -C-O-C_{symm} at 1010.33cm^{-1}, -C-O-C_{asymm} at 1264.21cm^{-1} respectively. After the complete analysis of different axially ligated [X-In-t(*p*-OCH_3)$_4$PP] complexes, we observed a little variation in the vibrational frequencies. For instance, in the IR spectrum of [SA-In-t(*p*-OCH_3)$_4$PP] (Fig. -2), vibrational frequencies appear at 2962.66cm^{-1} for aromatic -CH, 1398.39cm^{-1} for -CN, 1606.70cm^{-1} for -C=N, 1575.84cm^{-1} for -C=C, 1668.43cm^{-1} for -C=O, 1244.09cm^{-1} for -CO, 538.14cm^{-1} for In-N_{Por}, 667.37cm^{-1} for In-O_{SA} and –CH_{OCH3} vibrates at 2843.07cm^{-1}, 1016.49cm^{-1} for -C-O-C_{sym} and 1296.16cm^{-1} for -C-O-C_{asym} respectively whereas, in the IR spectrum of [5-ASA-In-t(*p*-OCH_3)$_4$PP] (Fig. 3), the vibrational frequencies appear at 2962.66cm^{-1} for aromatic -CH, 1384.89cm^{-1} for -CN, 1633.71cm^{-1} for -C=N, 1444.68cm^{-1} for -C=C, 1296.16cm^{-1} for -C-O, 520.78cm^{-1} for In-N_{Por}, 651.94cm^{-1} for In-O_{SA} and –CH group of the methoxy group attached at the periphery of the *meso*-phenyl ring vibrates at 2922.16cm^{-1}, 1012.63cm^{-1} for -C-O-C_{sym} and 1296.16cm^{-1} for -C-O-C_{asym} respectively and the $-NH_2$ group of the salicylate vibrates at 3213.41cm^{-1} for -NH_{2symm} and 3385.07cm^{-1} for -$NH_{2asym.}$

Table-1: UV-Visible Absorption Data of [X-In-t(*p*-OCH_3)$_4$PP] Complexes(X = substituted salicylates) in Different Solvents withλ_{max}, log ε, $\nu_{1/2}$ and '*f*' Values

Porphyrins	Solvent	B-bands λ_{max}(log ε), $\nu_{1/2}$ (nm), (dm^{3}M^{-1}cm^{-1}), (cm^{-1})	Q-bands λ_{max}(log ε), $\nu_{1/2}$ (nm), (dm^{3}M^{-1}cm^{1}),(cm^{-1})		Oscillator strength (f = 4.33 ×10^{-9}εΔ $\nu_{1/2}$)		
		B()0,0)			B()0,0)	Q-bands	
			Q1,0)	Q (0,0)		Q(1,0)	Q (0,0)
[SA-In- t(*p*-OCH_3)$_4$PP] [($C_7H_5O_3$)In($C_{44}H_{36}N_4O_4$)]	Acetone	439, (5.81), 730	573, (5.44), 670	605, (5.18)	2.047	0.604	0.412

				, 630			
	Dichloromethane	437, (5.77), 737	570, (5.42), 678	603, (5.17), 660	1.886	0.779	0.421
	Chloroform	435, (5.73), 799	564, (5.37), 793	601, (5.11), 663	1.874	0.810	0.367
[4-CSA-In- t(p-OCH_3)$_4$PP][($C_7H_4ClO_3$)In($C_{44}H_{36}N_4O_4$)]	Acetone	437, (4.95), 733	570, (4.56), 680	603, (4.30), 607	2.827	0.107	0.531
	Dichloromethane	434, (4.92), 740	567, (4.53), 717	601, (4.22), 636	2.655	0.105	0.465
	Chloroform	432, (5.91), 750	566, (4.50), 722	599, (4.10), 671	2.630	0.979	0.364
[5-CSA-In- t(p--OCH_3)$_4$PP][($C_7H_4ClO_3$)In($C_{44}H_{36}N_4O_4$)]	Acetone	435, (4.95), 679	568, (4.56), 714	606, (4.29), 630	0.259	0.118	0.537
	Dichloromethane	435, (4.91), 682	564, (4.52), 694	605, (4.20), 603	0.240	0.997	0.420
	Chloroform	432, (4.91), 802	564,(4.49),694	600, (4.06), 636	0.280	0.935	0.320
[4-ASA-In- t(p-OCH_3)$_4$PP][($C_7H_6NO_3$)In($C_{44}H_{36}N_4O_4$)]	Acetone	441, (5.64) 717	564, (5.30), 724	606, (5.03), 680	1.363	0.622	0.313
	Dichloromethane	440, (5.60), 777	563, (5.25), 687	604, (5.00), 581	1.344	0.527	0.252
	Chloroform	437, (5.60), 635	560, (5.24), 729	602, (5.00), 583	1.090	0.545	0.252
[5-ASA-In- t(p-OCH_3)$_4$PP][($C_7H_6NO_3$)In($C_{44}H_{36}N_4O_4$)]	Acetone	445, (5.64), 809	568, (5.29), 777	607, (5.06), 651	1.541	0.659	0.327
	Dichloromethane	442, (5.61), 717	564, (5.26), 754	605, (5.02), 656	1.254	0.595	0.302
	Chloroform	440, (5.60), 677	563, (5.24), 757	604, (4.99), 713	1.169	0.574	0.302
[5-FSA-In- t(p-OCH_3)$_4$PP][($C_7H_4FO_3$)In($C_{44}H_{36}N_4O_4$)]	Acetone	443, (4.86), 717	567, (5.49), 777	605, (4.24), 656	0.225	1.049	0.493
	Dichloromethane	441,(4.80),723	564, (4.47), 724	604, (4.19), 687	0.199	0.934	0.459
	Chloroform	437(4.77), 686	560, (4.44), 768	601, (4.05), 610	0.176	0.924	0.297
[5-SSA-In- t(p-OCH_3)$_4$PP][($C_7H_5O_6S$)In($C_{44}H_{36}N_4O_4$)]	Acetone	433(4.93), 750	566, (4.56), 784	602, (4.28), 634	0.281	0.123	0.052
	Dichloromethane	431(4.91),	565, (4.54),	600,	0.271	0.118	0.04

		768	782	(4.23), 638			7
	Chloroform	429(4.91), 747	563, (4.48), 760	598, (4.17), 642	0.262	0.100	0.089
[5-NSA-In- t(p-OCH_3)$_4$PP] [($C_7H_4NO_5$)In($C_{44}H_{36}N_4O_4$)]	Acetone	437(4.87), 635	569, (4.56), 682	600, (4.22), 584	0.207	0.107	0.042
	Dichloromethane	436, (4.88), 637	567, (4.52), 747	598, (4.11), 615	0.210	0.108	0.034
	Chloroform	433, (4.87), 802	566, (4.50), 749	595, (4.10), 705	0.256	0.103	0.038

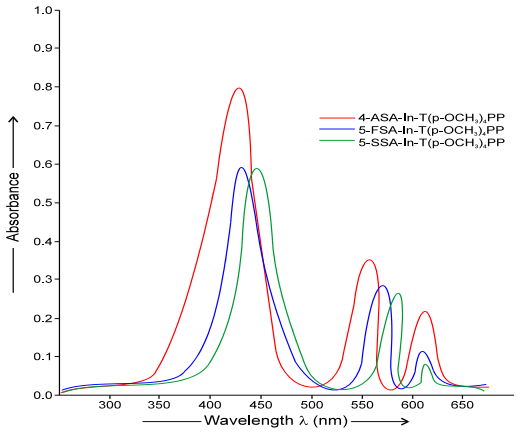

Fig.-1: Electronic Absorption Spectra of [4-ASA-In-t(p-OCH_3)$_4$PP], [5-FSA-In-t(p-OCH_3)$_4$PP], [5-SSA-In-t(p-OCH_3)$_4$PP] in Chloroform

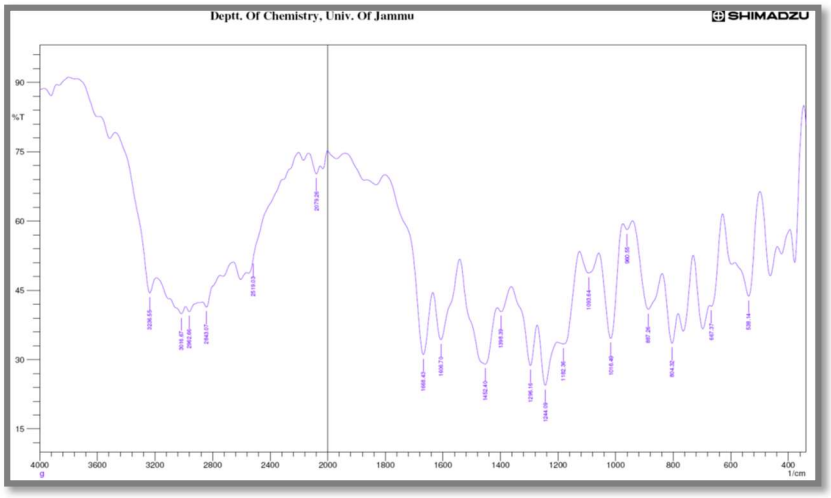

Fig.-2: Infra-red Spectrum of [SA-In-t(p-OCH_3)$_4$PP] in KBr Pellets

^{1}HNMR Spectroscopy

The free-base [H_2-t(p-OCH_3)$_4$PP] shows the characteristic resonance of imino-protons whereas these protons were absent in the In(III)porphyrins derivatives with axial ligands because of the incorporation of In(III) ion with the substitution of two imino protons from the porphyrin macrocycle center that results to the high field due to the strong shielding effect of the porphyrin ring. In the ^{1}HNMR spectrum of [5-ASA-In-t(p-OCH_3)$_4$PP] (Table-2), the $H_{\beta\text{-pyrrole}}$ protons resonate at 8.97ppm as a singlet whereas *meso*-aryl H_{ortho}

and H_{meta} protons resonate at 8.10ppm and at 7.64ppm as a doublet respectively. In addition to this, H_{OCH3} at the *meso*-position of the macrocycle resonates at 3.42ppm as a singlet. Also, the axially ligated aminosalicylate group protons resonate at 6.02ppm for H_3, 6.23ppm for H_4, and 6.61ppm for H_6, and -NH_2 protons resonate as a singlet at 9.51ppm.

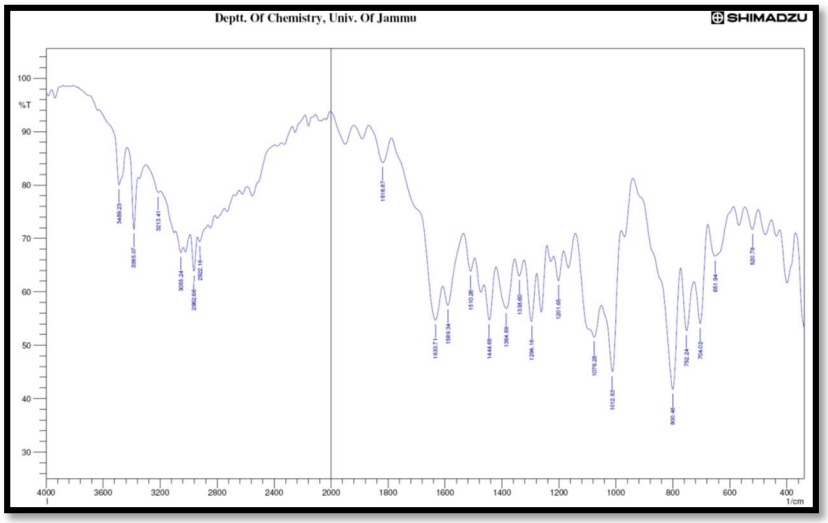

Fig.-3:Infra-red Spectrum of [5-ASA-In-t(p-OCH_3)$_4$PP] in KBr Pellets

In the case of [5-CSA-In-t(p-OCH_3)$_4$PP], the $H_{\beta\text{-pyrrole}}$ protons resonate at 9.00ppm as a singlet whereas H_{ortho} and H_{meta} protons resonate as doublets at 8.25ppm and 7.69ppm respectively. In addition, *meso*-methoxy protons resonate at 3.59ppm as a singlet, which is downfield as compared to [SA-In-t(p-OCH_3)$_4$PP]. Also, the protons of the 5-chlorosalicylate appear at 6.18ppm for H_3, 6.36ppm for H_4, and 6.71ppm for H_6. The ^{1}HNMR spectrum of [5-FSA-In-t(p-OCH_3)$_4$PP], reveals that the $H_{\beta\text{-pyrrole}}$ protons resonate at 9.09ppm as a singlet, the H_{ortho} and H_{meta} protons resonate at 8.18ppm and 7.71ppm as doublets respectively. The *meso*-methoxy protons resonate at 3.50ppm as a singlet which is also shifted deshielded as compared to [SA-In-t(p-OCH_3)$_4$PP]. The protons of the 5-fluoro salicylate molecule appear at 6.11ppm for H_3, 6.38ppm for H_4, and 6.72ppm for H_6. From the information obtained by studying the ^{1}HNMR data mentioned, it can be concluded that all the axially ligated [X-In-t(p-OCH_3)$_4$PP] show an upfield shifting of NMR signals as compared to the [In-t(p-OCH_3)$_4$PP], due to the nature of the organic moiety attached to the axially ligated salicylate anion that affected the position of NMR signals for all the synthesized complexes.

Table-2: ^{1}HNMR Data of [H_2-t(p-OCH_3)$_4$PP] and [X-In-t(p-OCH_3)$_4$PP] Complexes (X= substituted salicylates as axial ligands) Showing Chemical Shift Values at 298K

Porphyrins	β-Pyrrole Protons	N-H Protons	*meso*-aryl Protons	Other Protons
[H_2-t(p-OCH_3)$_4$PP] [$C_{48}H_{38}N_4O_4$]	8.79(8H, s)	-2.10	8.07(d, H_o), 7.23(d, H_m)	3.95 (s, 12H, -OCH_3)
[Cl-In- t(p-OCH_3)$_4$PP] [$C_{44}H_{36}N_4O_4ClIn$]	9.05(8H, s)	-	8.62(d, H_o), 7.40(d, H_m)	3.70 (s, 12H, -OCH_3)
[OH-In- t(p-OCH_3)$_4$PP] [$C_{44}H_{37}N_4O_5In$]	8.82(8H, s)	-	8.45(d, H_O), 7.89(d, H_m)	3.79 (s, 12H, -OCH_3)
[SA-In- t(p-OCH_3)$_4$PP] [($C_7H_5O_3$)In($C_{44}H_{36}N_4O_4$)]	8.91(8H, s)	-	8.18(d, H_o), 7.68(d, H_m)	6.15(d, $H_{3''}$), 6.30(t, $H_{4''}$), 6.41(t, $H_{5''}$), 6.72(d, $H_{6''}$), 3.74(s,12H,OCH_3)
[4-CSA-In- t(p-OCH_3)$_4$PP] [($C_7H_4ClO_3$)In($C_{44}H_{36}N_4O_4$)]	9.09(8H, s)	-	8.27(d, H_o), 7.70(d, H_m)	6.20(s, $H_{3''}$),6.39(d, $H_{5''}$),6.70(d, $H_{6''}$), 3.55(s,12H,OCH_3)

[5-CSA-In- t(*p*-$OCH_3)_4$PP] [($C_7H_4ClO_3$)In($C_{44}H_{36}N_4O_4$)]	9.00(8H, s)	-	8.25(d, H_o), 7.69(d, H_m)	6.18(d, $H_{3''}$), 6.36(d, $H_{4''}$), 6.71(s, $H_{6'}$), 3.59(s,12H,OCH_3)
[4-ASA-In- t(*p*-$OCH_3)_4$PP] [($C_7H_6NO_3$)In($C_{44}H_{36}N_4O_4$)]	9.03(8H, s)	-	8.12(d, H_o), 7.62(d, H_m)	6.05(s, $H_{3''}$),6.25(d, $H_{5''}$),6.59(d, $H_{6''}$),3.43(s,12H,OCH_3), 9.48(s, 2H,4-NH_2)
[5-ASA-In- t(*p*-$OCH_3)_4$PP] [($C_7H_6NO_3$)In($C_{44}H_{36}N_4O_4$)]	8.97(8H, s)	-	8.10(d, H_o), 7.64(d, H_m)	6.02(d, $H_{3''}$), 6.23(d, $H_{4'}$), 6.61(s, $H_{6''}$), 3.42(s,12H,OCH_3), 9.51(s, 2H,5-NH_2)
[5-FSA-In- t(*p*-$OCH_3)_4$PP] [($C_7H_4FO_3$)In($C_{44}H_{36}N_4O_4$)]	9.09(8H, s)	-	8.18(d, H_o), 7.71(d, H_m)	6.11(d, $H_{3''}$), 6.38(d, $H_{4''}$), 6.72(s, $H_{6''}$), 3.50(s,12H,OCH_3)
[5-SSA-In- t(*p*-$OCH_3)_4$PP] [($C_7H_5O_6S$)In($C_{44}H_{36}N_4O_4$)]	9.10(8H, s)	-	8.22(d, H_o), 7.74(d, H_m)	6.16(d, $H_{3''}$), 6.39(d, $H_{4''}$), 6.74(s, $H_{6''}$), 3.57(s,12H,OCH_3)
[5-NSA-In- t(*p*-$OCH_3)_4$PP] [($C_7H_4NO_5$)In($C_{44}H_{36}N_4O_4$)]	8.99(8H, s)	-	8.20 (d, H_o),7.69(d, H_m)	6.13(d, $H_{3''}$), 6.40(d, $H_{4''}$), 6.77(s, $H_{6''}$), 3.51(s,12H,OCH_3)

δ= Chemical shift(ppm); the pattern of peakssplitting represent by: (s = singlet, d = doublet, t = triplet, m= multiplet) and location and number of protons represents by: *o* = ortho: *p* = para: *m* = meta

^{13}CNMR Spectroscopy

Two major groups for carbon frequencies can be distinguished for the In(III) axially ligated porphyrin derivatives by the performance of ^{13}CNMR in which carbons of *meso*-tetraphenyl porphyrin ring resonate between 130ppm to 170ppm and the carbon for methine group at 90ppm to 150ppm region. The ^{13}CNMR spectrum of [H_2-t(*p*-$OCH_3)_4$PP] (Table-3) gives rise to the ^{13}C shifts at 134.8ppm for C_{meso}, 129.3ppm for $C_{3,5}$, 127.6ppm for C_4, 124.8ppm for C_β, 136.3ppm for $C_{2,6}$, and 142.3ppm for C_1 and a very broad signal at 138.0ppm for the α-carbon. It has been observed from the ^{13}CNMR spectrum that the existence of four electron-donating (–OCH_3) groups at the *para*-position of the [H_2-t(*p*-$OCH_3)_4$PP] causes a slight upfield(shielding) shift of the ^{13}C values. The ^{13}CNMR spectrum of [5-CSA-In-t(*p*-$OCH_3)_4$PP] shows peaks at 153.4ppm and 132.1ppm for C_α and C_β, 147.0ppm and 130.1ppm for C_1 and C_4, 135.2ppm and 128.3ppm for $C_{2,6}$ and $C_{3,5}$ and 124.0ppm for C_{meso} corresponding to the carbon atoms of the porphyrin ring. The peaks due 5-chlorosalicylate carbon atoms appear at 116.1ppm for $C_{4''}$, 121.5ppm for $C_{3''}$, 122.4ppm for $C_{5''}$, 132.4ppm for $C_{6''}$, 139.8ppm for $C_{2''}$, 158.2ppm for $C_{1''}$, 172.0ppm for C_{COO} and 64.9ppm for C_{OCH3}. The ^{13}CNMR spectrum of [5-ASA-In-t(*p*-$OCH_3)_4$PP]shows peaks at 152.8ppm and 132.4ppm for C_α and C_β, 146.5ppm and 130.7ppm for C_1 and C_4, 135.9ppm and 128.1ppm for $C_{2,6}$ and $C_{3,5}$ and 123.5ppm for C_{meso} corresponding to the carbon atoms of the porphyrin ring. The peaks due 5-aminosalicylate carbon atoms appear at 113.5ppm for $C_{4''}$, 117.5ppm for $C_{3''}$, 118.2ppm for $C_{5''}$, 124.8ppm for $C_{6''}$, 137.5ppm for $C_{2''}$, 154.1ppm for $C_{1''}$, 169.6ppm for $C_{COO}$and 64.4ppm for C_{OCH3}.

Table-3: ^{13}CNMR Data of [X-In-t(*p*-$OCH_3)_4$PP] Complexes (X = substituted salicylates as axial ligands) Showing Chemical Shift(δ in ppm) Values at 298 K

Porphyrins	C_α	C_β	C_1	C_4	$C_{2,6}$	$C_{3,5}$	C_{meso}	Salicylate Carbons						Other Groups	
								$C_{1''}$	$C_{2''}$	$C_{3''}$	$C_{4''}$	$C_{5''}$	$C_{6''}$	C_{COO}	C_{OCH3}
[SA-In-t(*p*-$OCH_3)_4$PP] [($C_7H_5O_3$)In($C_{48}H_{36}N_4O_4$)]	153.2	132.1	147.3	130.6	135.1	128.5	124.1	161.5	137.1	119.0	114.1	120.9	131.2	169.2	64.3

4-CSA-In- t(*p*-$OCH_3)_4$PP [$(C_7H_4ClO_3)In(C_{48}H_{36}N_4O_4)$]	153.5	132.6	147.6	130.5	135.7	128.2	124.8	158.4	139.5	121.9	116.5	122.7	132.1	172.4	64.8
5-CSA-In- t(*p*-$OCH_3)_4$PP [$(C_7H_4ClO_3)In(C_{48}H_{36}N_4O_4)$]	153.4	132.4	147.0	130.1	135.2	128.3	124.0	158.2	139.8	121.5	116.1	122.4	132.4	172.0	64.9
4-ASA-In- t(*p*-$OCH_3)_4$PP [$(C_7H_6NO_3)In(C_{48}H_{36}N_4O_4)$]	152.5	132.5	147.5	130.1	135.0	128.5	124.6	155.9	137.3	118.1	113.1	117.2	125.3	169.1	64.6
5-ASA-In- t(*p*-$OCH_3)_4$PP [$(C_7H_6NO_3)In(C_{48}H_{36}N_4O_4)$]	152.8	132.4	146.5	130.7	135.9	128.1	123.5	154.1	137.5	117.5	113.5	118.2	124.8	169.6	64.4
5-FSA-In- t(*p*-$OCH_3)_4$PP [$(C_7H_4FO_3)In(C_{48}H_{36}N_4O_4)$]	153.5	133.5	147.9	130.1	136.7	128.5	124.2	157.2	138.2	119.1	115.1	120.1	129.0	171.2	64.5
5-SSA-In- t(*p*-$OCH_3)_4$PP [$(C_7H_5O_6S)In(C_{48}H_{36}N_4O_4)$]	153.6	133.1	147.3	130.5	136.3	128.7	124.7	157.2	139.6	119.2	114.2	121.5	130.4	172.4	64.7
5-NSA-In- t(*p*-$OCH_3)_4$PP [$(C_7H_4NO_5)In(C_{48}H_{36}N_4O_4)$]	154.2	133.9	147.3	130.2	136.5	128.1	124.8	158.5	137.2	120.5	115.6	120.6	131.8	171.6	64.7

δ= Chemical shift(ppm); the pattern of peaks splitting represent by: (s = singlet, d = doublet, t = triplet, m= multiplet) and location and number of protons represents by: *o* = ortho: *p* = para: *m* = meta

Thermogravimetric and Differential Thermal Analysis

The simultaneous TGA/DTA study for the complex [5-SSA-In-t(*p*-$OCH_3)_4$PP] (Fig.-4) was carried out to observe the weight changes with the flow of heat as a function of temperature at controlled atmospheric pressure.[41,42]The TGA/DTA curve of the complex [5-SSA-In-t(*p*-$OCH_3)_4$PP]shows a constant loss in the weight beginning from 120°C to 850°C, till a stable nitride of indium(In-N_{por}) is formed at 800°C. The starting loss in weight of about 19.89% (the observed value = 20.38%) is observed at 150°C that may be attributed to the removal of the 5-sulfosalicylate group(5-SSA) which is axially ligated to tetra(*p*-methoxyphenyl)porphyrin In(III) supported by the exothermic peak at 130°C on the differential thermal curve. At 400°C, about 60.25% (the observed value = 60.57%) of the mass had been lost which corresponds approximately to the loss of four (*para*-methoxyphenyl) groups present at the periphery of the porphyrin ring. At 600°C, up to 84.31% (the theoretical value = 84.61%) of the total mass had been lost, correspondingly there is a large exothermic peak at 475°Con the DTA curve attributed to the elimination of four pyrrole groups. At 800°C, about 12.11% (against the theoretical value = 12.49%) of the total mass is left which is assigned to the Indium nitride present as a residue.

Elemental Analysis and Mass Analysis

The In(III)porphyrins axially ligated with different salicylate derivatives are readily soluble in solvents like $CHCl_3$, CH_2Cl_2,CH_3OH, and DMSO, which help in carrying out the analysis of different elements present in the complexes and mass analyticaldata as given in Table-4 and Fig.-5.

Fluorescence Spectroscopy

The emission bands of [H_2-t(*p*-$OCH_3)_4$PP] show red-shift at 664nm and 720nm as compared to the all axially ligated [In-t(*p*-$OCH_3)_4$PP], which exhibited two fluorescence bands with emission ranging 600nm to 700nm. However, for axially ligated In(III)porphyrin derivatives showing emission bands containing electron-donating groups are bathochromic or red-shifts whereas electron-withdrawing groups are

hypsochromic or blue-shifted in comparison to the metal-free porphyrin. It has also been observed that both the absorption and emission spectra are replicas of each other that dispense chief knowledge for the singlet excited state and optical properties respectively, which are forced by the existence of substituents (-OCH_3) group at *meso*-aryl positions of the macrocycle.[43]The fluorescence spectra of some representative complexes of [X-In-t(*p*-R)$_4$PP] in dichloromethane solvent are displayed in (Fig.-6) and their fluorescence data are summarized in (Table-5).

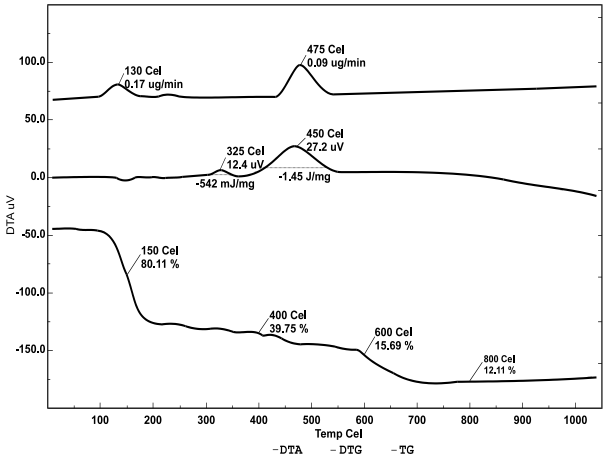

Fig.-4: TGA/DTA Curve of (*meso*-tetra-*p*-methoxyphenyl-porphyrinato)-5-sulfosalicylato-indium(III)[5-SSA-In-t(*p*-OCH_3)$_4$PP]

The tabulated data concluded that in axially ligated In(III)porphyrin complexes the emission bands are accompanied by bathochromic shifts with a variation in the intensity of the chromophores basic absorption bands for salicylates containing electron-donating groups due to the enhancement of electron density at the center of the porphyrin ring whereas, for salicylates containing electron-withdrawing groups, hypsochromic shift are observed.[44]In general, the observed fluorescence in *meso-para* phenyl substituted porphyrins is dependent on the structural changes in the excited state due to the torsion between the porphyrin, substituted phenyl group and on the extent of the electron-releasing ability of the porphyrins to form charge transfer state(ICT). Also, the changes observed in the emission bands in the substituted metal-free macrocycle, its metalled counterpart, and axially ligated derivatives prove that the steric effect is operative due to the presence of *para*-electron releasing and *para*-electron attracting groups in the porphyrin and must possess a considerable fraction of charge transfer in the excited state.

Table-4: Data for Mass Spectras(*m/z*) and Elemental Analysis For Axially Ligated [X-In-t(*p*-OCH_3)$_4$PP] Complexes (X = substituted salicylates as axial ligands)

Porphyrins	Mass Analytical Data (*m/z*)		Elemental Analysis (C, H, N, S %)							
	Calculated	Observed	Calculated				Observed			
			C	H	N	S	C	H	N	S
[SA-In- t(*p*-OCH_3)$_4$PP] [($C_7H_5O_3$)In($C_{48}H_{36}N_4O_4$)]	984.8	983.1	70.84	3.82	6.48	-	70.72	3.79	6.38	-
[4-CSA-In- t(*p*-OCH_3)$_4$PP] [($C_7H_4ClO_3$)In($C_{48}H_{36}N_4O_4$)]	1019.2	1019.2	68.12	3.67	6.23	-	68.11	3.65	6.46	-
[5-CSA-In- t(*p*-OCH_3)$_4$PP] [($C_7H_4ClO_3$)In($C_{48}H_{36}N_4O_4$)]	1019.2	1019.5	68.12	3.67	6.23	-	68.19	3.70	6.82	-
[4-ASA-In- t(*p*-OCH_3)$_4$PP] [($C_7H_6NO_3$)In($C_{48}H_{36}N_4O_4$)]	999.8	999.2	69.64	3.87	7.96	-	69.60	3.80	7.00	-
[5-ASA-In- t(*p*-OCH_3)$_4$PP] [($C_7H_6NO_3$)In($C_{48}H_{36}N_4O_4$)]	999.8	999.6	69.64	3.87	7.96	-	69.67	3.92	7.53	-
[5-FSA-In- t(*p*-OCH_3)$_4$PP] [($C_7H_4FO_3$)In($C_{48}H_{36}N_4O_4$)]	1002.7	1003.2	69.40	3.62	6.35	-	69.32	3.55	6.42	-

[5-SSA-In- t(p-OCH_3)$_4$PP] [($C_7H_5O_6S$)In($C_{48}H_{36}N_4O_4$)]	1064.8	1080.3	64.84	3.52	5.93	3.39	64.79	3.57	5.91	3.52
[5-NSA-In- t(p-OCH_3)$_4$PP] [($C_7H_4NO_5$)In($C_{48}H_{36}N_4O_4$)]	1029.7	1030.5	67.34	3.85	7.70	-	67.30	3.91	7.95	-

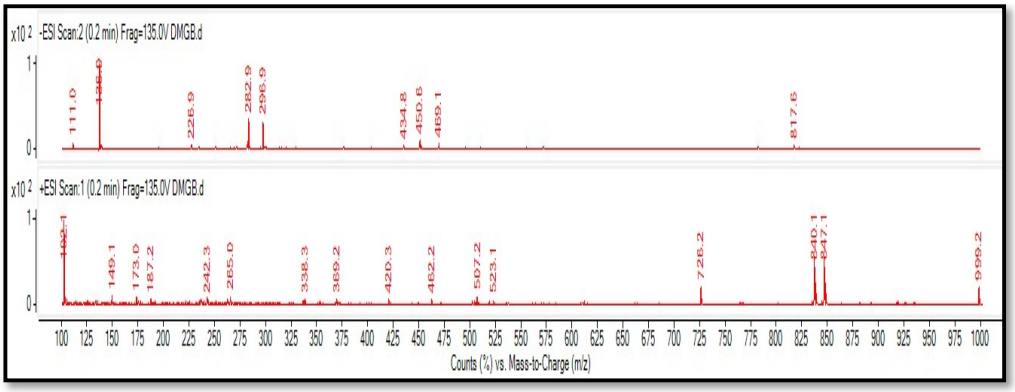

Fig.-5: Mass Spectrum of [4-ASA-In-t(p-OCH_3)$_4$PP]

Table-5: Data for Emission Spectra of [X-In-t(p-OCH_3)$_4$PP] Complexes(X= substituted salicylates as axial ligands) at 298K in Dichloromethane Using at 550nm

Porphyrins	λ_{max}, nm	
	Q(0,0)	Q(1,0)
[H_2-t(p-OCH_3)$_4$PP][$C_{48}H_{38}N_4O_4$]	664	720
[Cl-In- t(p-OCH_3)$_4$PP][$C_{48}H_{36}N_4O_4ClIn$]	587	625
[OH-In-t(p-OCH_3)$_4$PP][$C_{48}H_{37}N_4O_5In$]	598	626
[SA-In-t(p-OCH_3)$_4$PP][($C_7H_5O_3$)In($C_{48}H_{36}N_4O_4$)]	591	630
[4-CSA-In-t(p-OCH_3)$_4$PP][($C_7H_4ClO_3$)In($C_{48}H_{36}N_4O_4$)]	589	629
[5-CSA-In-t(p-OCH_3)$_4$PP][($C_7H_4ClO_3$)In($C_{48}H_{36}N_4O_4$)]	589	630
[4-ASA-In-t(p-OCH_3)$_4$PP][($C_7H_6NO_3$)In($C_{48}H_{36}N_4O_4$)]	591	632
[5-ASA-In-t(p-OCH_3)$_4$PP][($C_7H_6NO_3$)In($C_{48}H_{36}N_4O_4$)]	591	631
[5-FSA-In-t(p-OCH_3)$_4$PP][($C_7H_4FO_3$)In($C_{48}H_{36}N_4O_4$)]	590	630
[5-SSA-In-t(p-OCH_3)$_4$PP][($C_7H_5O_6S$)In($C_{48}H_{36}N_4O_4$)]	589	630
[5-NSA-In-t(p-OCH_3)$_4$PP][($C_7H_4NO_5$)In($C_{48}H_{36}N_4O_4$)]	598	627

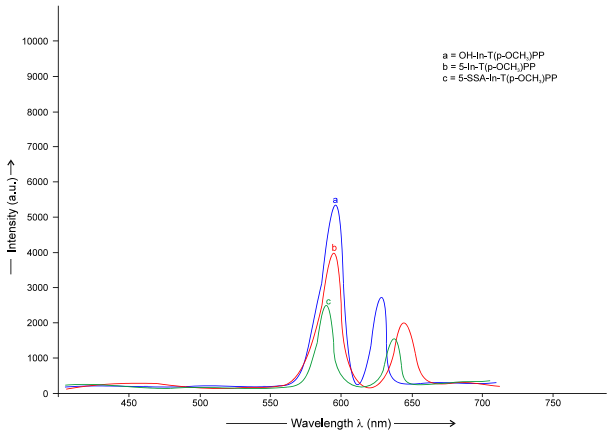

Fig.-6: Fluorescence Emission Spectra of (a) [OH-In-t(p-OCH_3)$_4$PP] (b) [5-CSA-In-t(p-OCH_3)$_4$PP] (c) [5-SSA-In-t(p-OCH_3)$_4$PP] in dichloromethane at 550nm

Cyclic Voltammetry

Cyclic Voltammetry (CV) studies revealed that, 1. Identity and oxidation number of the central metal ion, 2. Type and number of axially coordinated ligands, and 3. Type and planarity of the conjugated macrocycle. The CV studies for the [H_2-t(p-OCH_3)$_4$PP] complex show two electron reduction-oxidation

processes in CH_2Cl_2. The values obtained for axially ligated [X-In-t(p-OCH_3)$_4$PP] are quite close to those of the corresponding monomeric metal free [H_2-t(p-OCH_3)$_4$PP] and it's metallated [In-t(p-OCH_3)$_4$PP] porphyrins complexes. The metallated [Cl-In-t(p-OCH_3)$_4$PP] precursor undergoes two-electron reversible reductions in $CH_2Cl_2$with 0.1M (TBA)PF_6 and the difference in potential is 0.35V, which shows that the addition of electrons in the macrocycle π-system that led to the formation of a dianion and a radical species. The dissociation of the Cl^- ion from the complex occurs after the electro reduction of [Cl-In-t(p-OCH_3)$_4$PP] whereas the electro-oxidation of [Cl-In-t(p-OCH_3)$_4$PP] is complicated in $CH_2Cl_2$with 0.1M (TBA)PF_6, which shows three reversible oxidations in which the first step include the two-electrons transfer reaction whereas the second and third step include the transfer of single-electron. It has also been observed that there is a reduction peak by two-electron transfer which may be attributed to the equilibrium that exists within the In(III)porphyrin and the anionic component of the reference electrolyte, or may be due to the–Cl ion oxidation, or by the oxidation of the one or more porphyrin decomposition products. The cyclic voltammograms for axially ligated [5-FSA-In-t(p-OCH_3)$_4$PP] (Fig.-7) and [5-NSA-In-t(p-OCH_3)$_4$PP] (Fig.-8) complexes are occur through two one-electron transfer reactions. All the observed values are in good agreement with 0.42±0.05V separation which is generally noted for π-ring centered reductionprocesses.[45-47]Also, the potentials due to oxidation and the complete electrochemical nature of In(III)porphyrin complexes depend on the suitable solvent/supporting electrolyte system. With CH_2Cl_2 solution, [X-In-t(p-OCH_3)$_4$PP] complexes undergo two-electron oxidations corresponding to M^+/M^{2+} and M^{2+}/M^{3+}. The observations and the data available from the literature suggested that chemical reactions involved in the oxidation-reduction of In(III) porphyrins follow the first one-electron oxidation with the removal of X group from the complex and form the [In-t(p-OCH_3)$_4$PP]$^+$, as follow:[48]

$$\mathbf{X\text{-}M\text{-}T(p\text{-}R)_4PP} \overset{e^-}{\rightleftharpoons} \mathbf{X\text{-}M\text{-}[T(p\text{-}R)_4PP]^{\cdot+}} \longrightarrow \mathbf{[M\text{-}T(p\text{-}R)_4PP)]^+ + X^-} \qquad (1)$$

The second oxidation of [X-In-t(p-OCH_3)$_4$PP]involves the changes in the substituted axial ligand and led to the generation of [In-t(p-OCH_3)$_4$PP]$^{2+}$ species as shown in the below equation:

$$\mathbf{[X\text{-}M\text{-}(T(p\text{-}R)_4PP)]^{\cdot+}} \rightleftharpoons \mathbf{[M\text{-}(T(p\text{-}R)_4PP)]^{2+} + e^-} \qquad (2)$$

$$\mathbf{[X\text{-}M\text{-}(T(p\text{-}R)_4PP)]^{\cdot 2+}} \rightleftharpoons \mathbf{[M\text{-}(T(p\text{-}R)_4PP)]^{3+} + e^-} \qquad (3)$$

Thus, to conclude it can be summarized that the porphyrins and metalloporphyrins show two reversible one-electron ring oxidations and reductions, which can be represented as:-

$$MP^{2+} \overset{-e^-}{\longleftrightarrow} MP^{+} \overset{-e^-}{\longleftrightarrow} MP \overset{+e^-}{\longleftrightarrow} MP^{-} \overset{+e^-}{\longleftrightarrow} MP^{2-}$$

These redox potentials are affected by the substituents present in the porphyrin periphery and also the presence of the electron-donating group facilitates oxidation that hinders reduction either at the center of the macrocycle π-system, whereas the existence of the electron-withdrawing group reduces the electron density from the porphyrin core and yield easier reductions and harder oxidations. Several investigations have been carried out on the redox potentials of the porphyrins due to the presence of different substituents at the periphery and the oxidation-reduction data are referenced against Ag/AgCl couple. For instance, the complex [5-FSA-In-t(p-OCH_3)$_4$PP] (Fig.-7) exhibits two reversible one-electron ring reduction and oxidation processes at 0.38V, 1.09V, and -0.68V, -1.27V respectively whereas the complex [5-NSA-In-t(p-OCH_3)$_4$PP] (Fig.-8) exhibits two reversible one-electron ring reduction and oxidation processes at 0.73V, 1.44V and -0.32V, -0.86V respectively. Thus, these results show that the effect of substituting *meso*-methoxy group of the porphyrin ring does not cause drastic effects on redox potentials of the metalloporphyrin complexes and also the presence of axially ligated electron-donating/electron-withdrawing substituted salicylate anion shifts the ring oxidation and reductions to a more anodic potential relative to that found for *p*-substituted [H_2-t(p-OCH_3)$_4$PP] /or [HO-In-t(p-OCH_3)$_4$PP] metallated porphyrin. Also, for the electron-donating (5-NSA) and (5-FSA) salicylate ions as axial ligands, the effect is more pronounced in ring reductions than oxidations in the case of (5-NSA) as compared to (5-FSA).

Antifungal Activity

The In(III)porphyrin complexes with axial ligands have been investigated for *invitro* activity against the microbe, *Acremonium fusidoides spp.* using the agar plate technique with potato dextrose agar (PDA) as nutrient medium.[49-5

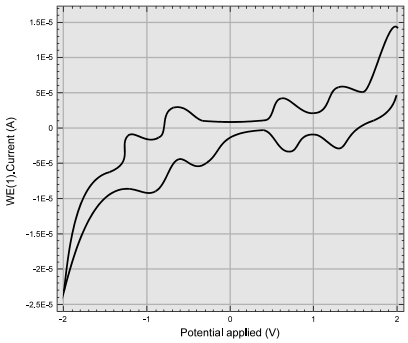

Fig.-7: Cyclic Voltammogram of [5-FSA-In-t(*p*-OCH_3)$_4$PP]

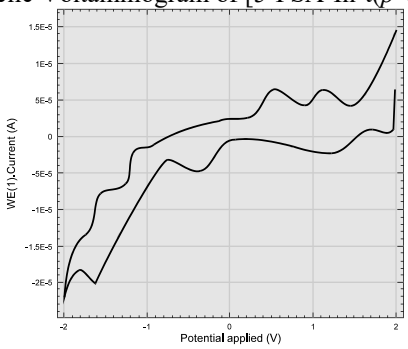

Fig.-8: Cyclic Voltammogram of [5-NSA-In-t(*p*-OCH_3)$_4$PP]

[2]On the basis of analysis, the fungus shows a linear growth at different concentrations over control and treatment and this linear growth can be calculated using equation-(A):

$$\text{Percentage Inhibition (I\%)} = [(C-T)/C] \times 100 \quad \text{(A)}$$

I= *Invitro* percentage inhibition,
C= total fungus growth (mm) in control, and
T= total fungus growth (mm) in treatment.

From the data (Table-6 and Fig.-9), it was shown that there is a decrease in the diameter of the fungal colony as the concentration of the complexes increases which results in the increase of percentage inhibition (I%). This is due to the fact that In(III)porphyrin complex diffuses in the fungal membrane either as a complete through the cell membrane of the fungus or through the integrating results of the In(III) as a metal ion, axial ligands/or the metalloporphyrin as a whole. This increase in activities can be elucidated by overtone's concept and tweedy's chelation theory[53-58], which explained that the distinction in the behavior of the fungus in opposition to In(III)porphyrin complexes is either dependent on cell membrane impermeability that approbates the transit of fat-soluble molecules for which the lipophilicity became an essential criterion that direct the antifungal activity. Also, the chelation of the metal ion with different substituents on the axial ligands will be reduced by the polarity of the metal ion due to the incomplete overlapping of the metal ion orbitals with the ligand orbitals.

Table-6: *Invitro* Antifungal Evaluation Data of [X-In-t(*p*-OCH_3)$_4$PP] Complexes Against *Acremonium fusidoides spp.*, C*=53mm

S.No.	Porphyrins	Complex Concentration (ppm)	Fungus Colony diameter (mm)	Percentage Inhibition *(I%) =[(C-T)/C] x 100*
1.	[5-SSA-In-t(*p*-OCH_3)$_4$PP] [($C_7H_5O_6S$)In($C_{48}H_{36}N_4O_4$)]	100	19	45.6
		200	12	52.9
		300	8	79.5
2.	[SA-In-t(*p*-OCH_3)$_4$PP] [($C_7H_5O_3$)In($C_{48}H_{36}N_4O_4$)]	100	22	46.81
		200	16	65.95
		300	9.2	80.42
3.	[5-ASA-In-t(*p*-OCH_3)$_4$PP]	100	25	64.15

	$[(C_7H_6NO_3)In(C_{48}H_{36}N_4O_4)]$	200	19	77.36
		300	13	84.90

*Total fungal colony diameter

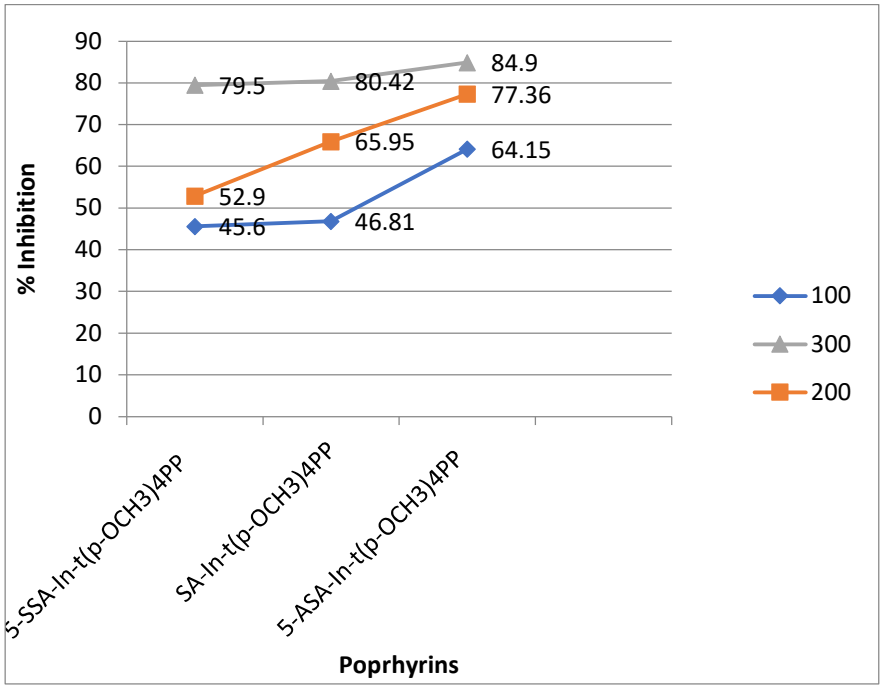

Fig.-9: *Invitro* Antifungal Activity (% Inhibition) of [5-SSA-In-t(p-OCH_3)$_4$PP]; [SA-In-t(p-OCH_3)$_4$PP]; and [5-ASA-In-t(p-OCH_3)$_4$PP] respectively by PDA Method

Antioxidant Activity

The investigation of possible antioxidant activities (Radical Scavenging Activity) (RSA) of substituted salicylates axially coordinated with In(III)porphyrin was determined as a DPPH radical discoloration percentage using 1,1-Diphenyl-2-picrylhydrazyl (DPPH) assay as equation-B:[59,60]

$$\%RSA = \frac{(A_o - A_s)}{A_o} \times 100 \qquad (B)$$

A_0= absorbance of the control, and
A_s = absorbance of the test complexes.

It is noticeable from the results (Table-7) that the free-radical antioxidant activities of these complexes depended on the absorbance and concentration as well (Fig.-10). Among the investigated complexes, the unsubstituted (OH-In-tMP) complex does not show any enhanced DPPH activity because of the absence of substituted salicylate ligands but as soon as substituted salicylates like (5-CSA), (5-ASA) and (5-FSA) coordinated with In(III) metal ion, variation in the DPPH activity was observed, expressed in EC_{50} value. The complex [5-ASA-In-tMP] shows maximum free-radical scavenging activity of about 37.23% followed by 31.91% for the [5-CSA-In-tMP] complex whereas the least activity was observed at 19.72% for [5-FSA-In-tMP] complex. All these observed variations in the substituted axially ligated In(III)porphyrin were based on the fact that phenolic, salicylic acids and their derivatives like compounds are considered excellent free-radical scavengers (powerful antioxidants), which can play an efficient character in controlling diseases due to oxidative stress that potentially interact with biological systems.[61-65]Chang and others 2001; Guleria and others 2010 explained that polyphenols play multifaceted antioxidant activity which is highly related to the electron trap capacity of the phenol ring to hunt species like superoxide, peroxy, and other oxygen-containing radicals. It has also been explored that in vegetable life, phenolic-like compounds are commonly found where they show their multiple biological effects

related to redox properties like proton donors, singlet oxygen quenchers, and reducing agents that proved their antioxidant activities.

Table-7: Data for Radical Scavenging Activity (%RSA) of Axially Ligated [X-In-t(p-OCH_3)$_4$PP] Complexes Using DPPH Method

S.No.	Porphyrins	Concentration (µl/ml)	Absorbance (A_s)	%RSA=$\frac{(A_o-A_s)}{A_o}$ ×100
1.	[OH-In-t(p-OCH_3)$_4$PP] [OH-In-tMP] [$C_{48}H_{37}N_4O_5In$]	50	1.006	9.3
		100	1.001	11.43
		200	0.981	15.52
2.	[5-CSA-In-t(p-OCH_3)$_4$PP] [5-CSA-In-tMP] [($C_7H_4ClO_3$)In($C_{48}H_{36}N_4O_4$)]	50	0.945	19.45
		100	0.885	27.58
		200	0.832	31.91
3.	[5-ASA-In-t(p-OCH_3)$_4$PP] [5-ASA-In-tMP] [($C_7H_6NO_3$)In($C_{48}H_{36}N_4O_4$)]	50	1.234	22.67
		100	0.995	27.58
		200	0.767	37.23
4.	[5-FSA-In-t(p-OCH_3)$_4$PP] [5-FSA-In-tMP] [($C_7H_4FO_3$)In($C_{48}H_{36}N_4O_4$)]	50	1.205	17.54
		100	1.119	18.08
		200	1.069	19.72

(A_o (absorbance of the control) = 1.222)

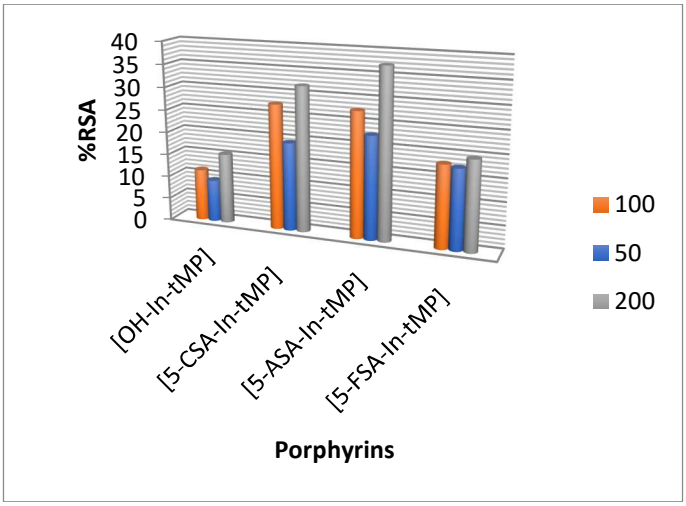

Fig.-10: Antioxidant Activity (%RSA) of Axially Ligated [5-FSA-In-tMP], [5-ASA-In-tMP], [5-CSA-In-tMP] and [5-FSA-In-tMP] respectively by DPPH Method

CONCLUSION

The research article explained the synthesis of In(III)porphyrins complexes axially ligated with substituted salicylates. The proposed structure (Fig.-11) of the In(III)porphyrin complexes was analyzed and characterized by electronic absorption, Infra-red, ^{1}HNMR, ^{13}CNMR, elemental analysis, mass spectroscopy, TGA/DTA, cyclic voltammetry, and biological activities. The electronic absorption spectra correspond to the change in the absorption wavelength and concomitant electronic coupling of the different salicylate ligands with porphyrin via In(III) metal ion. The Infrared vibrational frequencies confirmed the appearance of In-O_{SA} forming In(III)porphyrins complexes with five-coordinate geometry. Further, the ^{1}HNMR spectral study of the representative complexes showed that protons signals are shifted to the higher field for axially ligated In(III)porphyrins in comparison to the metal-free porphyrin macrocyclic ring. The mass spectroscopy confirmed the mass of the synthesized complexes as m/z ratio whereas ^{13}CNMR spectra confirms the resonance of the *meso*-carbon of porphyrin between 130ppm to 160ppm and the salicylate ring carbons between 110ppm to 165ppm. CV studies revealed the formation

of π-anion or cation radicals through two one-electron-transfer steps. The *in-vitro* antifungal activity(%inhibition) of In(III)porphyrin complexes shows the increase in percentage inhibition with the decrease in colony diameter and increase in the concentration of the complexes, whereas free radical scavenging(%RSA) reveals that these complexes were absorbance and concentration-dependent.

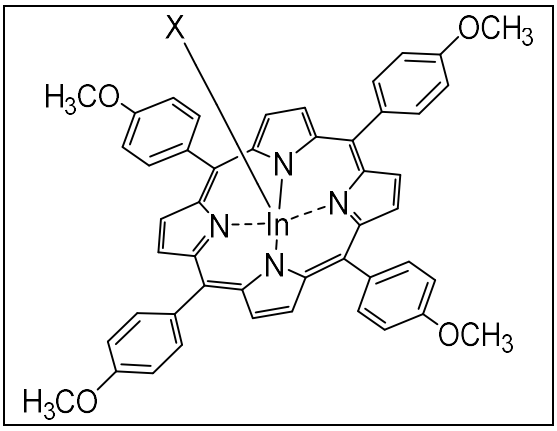

Fig.-11: Proposed Structure for the Axially Ligated In(III)-*meso*-porphyrin

ACKNOWLEDGMENTS

The authors acknowledge the Department of Chemistry, the University of Jammu for carrying out the TG/DTA and Cyclic Voltammetry studies respectively, and the Department of Biotechnology, the University of Jammu for carrying out the biological evaluation (antifungal activity and radical scavenging activity) of the In(III)porphyrin complexes.

CONFLICT OF INTERESTS

The authors declare that there is no conflict of interests.

AUTHOR CONTRIBUTIONS

All the authors contributed significantly to this manuscript, participated in reviewing/editing, and approved the final draft for publication. The research profile of the authors can be verified from their ORCID ids, given below:

D. Sharma https://orcid.org/0000-0002-0931-1169
D. Gupta https://orcid.org/0000-0002-0205-0971
S. Kundan https://orcid.org/0000-0001-8665-3667
G. D. Bajju https://orcid.org/0000-0002-6143-8853
S. Ravichandran https://orcid.org/0000-0001-7281-2778

REFERENCES

1. S. M. Korobkov, K. P. Birin, Y. G. Gorbunova and A. Yu. Tsivadze, *Dyes and Pigments*, **207**, 110696(2022), https://doi.org/10.1016/j.dyepig.2022.110696
2. K. P. Birin, Y. G. Gorbunova, A. Yu. Tsivadze, A. G. B. Lemeune and R. Guilard, *European Journal of Organic Chemistry*, **25**, 5610(2015), https://doi.org/10.1002/ejoc.201500628
3. A. Wiehe, Y. M. Shaker, J. C. Brandt, S. Mebs and M. O. Senge, *Tetrahedron*, **61(23)**, 5535(2005), https://doi.org/10.1016/j.tet.2005.03.086
4. K. P. Birin, I. A. Abdulaeva, D. A. Polivanovskaia, A. G. Martynov, A. V. Shokurov, Y. G. Gorbunova and A. Yu. Tsivadze, *Dyes and Pigments*, **186**, 109042(2021), https://doi.org/10.1016/j.dyepig.2020.109042

5. R. L. Brookfield, H. Ellul and A. Harriman, *Journal of Photochemistry*, **31(1)**, 97(1985), https://doi.org/10.1016/0047-2670(85)85077-2
6. K. P. Birin, A. I. Poddubnaya, I. A. Abdulaeva, Y. G. Gorbunova and A. Yu. Tsivadze, *Dyes and Pigments*, **156**, 243(2018), https://doi.org/10.1016/j.dyepig.2018.04.009
7. F. R. Kooriyaden, S. Sujatha, B. Varghese and C. Arunkumar, *Journal of Fluorine Chemistry*, **170**,10(2015), https://doi.org/10.1016/j.jfluchem.2014.11.007
8. Y. Yang. G. Li, Xi. Mao and Y. She, *Organic Process Research & Development*, **23(5)**, 1078(2019), https://doi.org/10.1021/acs.oprd.9b00030
9. M. S. Kumar, P. Aruna1 and S. Ganesan, *Rasayan Journal of Chemistry,* **12(3)**,1027(2019), http://dx.doi.org/10.31788/RJC.2019.1235149
10. M. O. Senge, M. Fazekas, E. G. A. Notaras, W. J. Blau, M. Zawadzka, O. B. Locos and E. M. Ni. Mhuircheartaigh, *Advanced Material*, **19**, 2737(2007), https://doi.org/10.1002/adma.200601850
11. G. O. N. Ndjawa, M. R. Tchalala, O. Shekhah, J. I. Khan, A. E. Mansour, J. C. Jóźwiak, L. J. Weselinski, H. A. Ahsaine, A. Amassian and M. Eddaoudi, *Materials*, **12**, 2457(2019), https://doi.org/10.3390/ma12152457
12. A. Varotto, L. Todaro, M. Vinodu, J. Koehne, G. Y. Liub and C. M. Drain, *Chemistry Communiation*, **40**, 4921(2008), https://doi.org/10.1039/B806795C
13. O. Horvath, R. Huszank, Z. Valicsek and G. Lendvay, *Coordination Chemistry Review*, **250**, 1792(2006), https://doi.org/10.1016/j.ccr.2006.02.014
14. Z. Valicsek, O. Horvath and K. L. Stevenson, *Photochemical Photobiology Science*, **3**, 669(2004), https://doi.org/10.1039/B405105J
15. K. M. Kadish, K. Smith and R. Guillard, The Porphyrin Handbook-Bioinorganic and Bioorganic Chemistry. Academic, New York, **1**, (2003), https://doi.org/10.1016/C2009-0-22714-0
16. H. Alyousef, B. M. Alotaibi, M. B. Yahia, M. M. Alanazi and N. A. Alsaif, *State Standard of the People's Republic of China*, Scientific Reports, **11**, 8316(2021).
17. S. Otieno, A. E. Lanterna, J. Mack, S. Derese, E. K. Amuhaya, T. Nyokong and J. C. Scaiano, *Molecules*, **26**, 3131(2021), https://doi.org/10.3390/molecules26113131
18. H. Darmokoesoemo, H. Setyawati, A. T. A. Ningtyas and H. S. Kusuma, *Rasayan Journal Chemistry,* **10(2)**, 313(2017), http://dx.doi.org/10.7324/RJC.2017.1021561
19. C. P. Wang, R. F. Venteicher and W. D. Horrocks Jr, *Journal of American Chemical Society*, **96**, 7149(1974), https://doi.org/10.1021/ja00829a079
20. J. E. Rogers, K. A. Ngugen, D. C. Hufnagle, D. G. Mcleam, W. Su, K. M. Gossett, A. R. Burke, S. A.Vinogradov, R. Pachter and P. A. Fleitz, *Journal of Physical Chemistry A*, **107**, 11331(2003), https://doi.org/10.1021/jp0354705
21. Y. Inokuma and A. Osuka, *Organic Letter*, **6**, 3663(2004), https://doi.org/10.1021/ol048953f
22. E. F. Cosma, C. Enache, R. Tudose, I. Armeanu, E. Mosoarca, D. Vlascici and O. Costisor, *Review Chimca*, **58**, (2007), https://doi.org/10.1016/j.arabjc.2014.10.011
23. S. Nadeem, F. Uddin, M. I. A. Mutalib and M. S. Shaharun, *Organic and Biochemistry*, **9**, 309(2022), https://doi.org/10.52568/001119/JCSP/44.05.2022
24. J. M. Perry, K. Mansour, I. Y. S. Lee, X. L. Wu, P. V. Bedworth, C. T. Chen, D. Ng, S. R. Marder, T. Wada, M. Tian and H. Sasabe, *Science*, **273**, 1533(1996), https://doi.org/10.1126/science.273.5281.1533
25. S. K. Sahoo, R. K. Bera, M. Baral and B. K. Kanungo, *Acta Chimica Slovenica*, **55**, 243(2008),
26. K. Ni, D. Liu, Z. Li, Z. Xiao, J. Yang and Y. Song, *Proceedings: International Symposium on Optoelectronic Technology and Application*, **92971N**, (2014), https://doi.org/10.1117/12.2073005
27. Y. H. Zhang, D. M. Chen, T. He and F. C. Liu, *Spectrochimica Acta Part A*, **59**, 87(2003), https://doi.org/10.1016/S1386-1425(02)00124-5
28. S. G. Ang, H. G. Ang, W. Han, B. W. Sun, M. K. Y. Lee, Y. W. Lee and G. Y. Yang, *Proceedings: Linear and Nonlinear Optics of Organic Materials II*, **4798**, 195(2002), https://doi.org/10.1117/12.451927
29. A. L. Abuhijleh and C. Woods, *Inorganic Chemical Communication*, **4**, 119(2001), https://doi.org/10.1016/S1387-7003(00)00221-5

30. J. L. Joyave, L. S. Steinhauer, D. L. Dillehay, C. K. Born and M. E. Hamrick,_*Biochemical Pharmacology,* **34**, 3915(1985), https://doi.org/10.1016/0006-2952(85)90444-7
31. V. Stavila, J. H. Thurston and K. H. Whitmire, *Inorganic Chemistry,* **48**, 6945(2009), https://doi.org/10.1021/ic9010357
32. J. H. Thurston, E. M. Marlier and K. H. Whitmire, *Chemical Communication*, **23**, 2834(2002), https://doi.org/10.1039/B209188G
33. N. G. Charles, E. A. H. Griffith, P. F. Rodesiler and E. L. Amma, *Inorganic_Chemistry*, **22**, 2717(1983), https://doi.org/10.1021/ic00161a016
34. E. Mieczynska, A. M.Trzeciak, J. J. Ziolkowski and T. Lis, *Polyhedron*, **13**, 655(1994), https://doi.org/10.1016/s0277-5387(00)84742-7
35. P. S. Pavacik, J. C. Huffman and G. Christou, *Chemical Communication*, **43**, (1986), https://doi.org/10.1039/C39860000043
36. J. B. Vincent, K. Folting, J. C. Huffman and G. Christou, *Inorganic Chemistry*, **25**, 996(1986), https://doi.org/10.1021/ic00227a022
37. D. Voet and J. G. Voet, Biochemistry, 4th edn. Wiley: New York, USA, (2004).
38. K. M. Kadish, K. M. Smith and R. Guilard, Modern Aspects of Porphyrinoid Chemistry, 46th edn. World Scientific Publishing Co: Singapore, 356(2022).
39. A. D. Adler, F. R. Longo, J. D. Finarelli, J. Goldmacher, J. Assour and L. Korsakoff, *Journal of Organic Chemistry*, **32**, 476(1967), https://doi.org/10.1021/jo01288a053
40. M. Bhatti, W. Bhatti and E. Mast, *Journal of Inorganic and Nuclear Chemistry*, **8(2)**, 113(1972).
41. X. Wei, D. Chen, X. Du and Z. Chen, *Thermochimica Acta*, **440**, 18(2006), https://doi.org/10.1016/j.tca.2005.10.017
42. V. H. A. Pinto, D. C. Da-Silva, J. L. M. S. Santos, T. Weitner, M. G. Fonsica, M. I._Yoshida, Y. M. Idemori and I. B. Haberle, *Journalof Pharmaceuticaland Biomedical Analysis*, (2012).
43. J. B. Kim, J. J. Leonard and R. F. Longo, *Journal of American Chemical Society*, **94**, 3986(1972), https://doi.org/10.1021/ja00766a056
44. S.V. Zaitzeva, S. A. Zdanowich, T. A. Ageeva, A. S. Ocheretovi and O. A. Golubchikov, *Molecules*, **5**, 786(2000), https://doi.org/10.3390/50600786
45. R. Guilard and K. M. Kadish, *Chemistry Review*, **88**, 1121(1988), https://doi.org/10.1021/cr00089a007
46. R. Guilard, C. Lecomte and K. M. Kadish, *Structure and Bonding*, **64**, 205(1987), https://doi.org/10.1007/BFb0036792
47. J. H. Fuhrhop, K. M. Kadish and D. G. Davis, *Journal of American Chemical Society*,_**95**, 5140(1973), https://doi.org/10.1021/ja00797a008
48. C. Di. Natale, R. Paolesse and A. D.Amico, *Journal of Porphyrin & Phthalocyanin*, **13(11)**, 1123(2009), https://doi.org/10.1142/S1088424609001443
49. G. Tortora, M. E. Ryan, H. M. Lee and L. M. Golub, *Antimicrobial Agents Chemotherapy*, **46(5)**, (2002), https://doi.org/10.1128/AAC.46.5.1447-1454.2002
50. S. Magaldi, M. Essayag, C. H. De Capriles, C. Perez, M. T. Colella, C. Olaizola and Y. Ontiveros, *International Journal of Infectious Diseases,* **8(1)**, 39(2004), https://doi:10.1016/j.ijid.2003.03.002
51. S. A. Kermani, S. Salari and P. G. N. Almani, *Journal of Clinical Laboratory Analysis*, **35(1)**, (2021), https://doi.org/10.1002/jcla.23577
52. S. F. Yusoff, F. F. Haron, M. T. M. Mohamed, N. Asib, S. Z. Sakimin, F. A. Kassim and S.I.Ismail, *Biology*, **11(2)**, 373(2021), https://doi.org/10.3390/argonomy11020373
53. B. B. Beyene, M. M. Ayenew and T. A. Amogne, *Results in Chemistry*, **2**, 100073(2020), https://doi.org/10.1016/j.rechem.2020.100073
54. S. Belaid, A. Landreau, S. Djebbar, O. B. Baitich, G. Bouet and J. P. Bouchara, *Journal of Inorganic Biochemistry*, **102**, 63(2008), https://doi.org/10.1016/j.jinorgbio.2007.07.001
55. A. Ahmed, A. A. Al-Amiery, A. A. H. Abdul, A. H. Kadhum and_A. B. A. B. Mohammad, *Molecules*, **17**, 5713(2012), https://doi.org/10.3390/molecules17055713
56. A. Adesra and V. K .Srivastava, *Future Journal Pharmaceutical Science*, **61**, 270(2021), https://doi.org/10.1007/s12088-021-00943-5

57. S. Omidi and A. Kakanejadifard, *The Royal Society of Chemistry Advances*, **10**, 30186(2020), https://doi.org/10.1039/D0RA05720G
58. F. I. Abouzayed, S. A. Abouel-Eneinand and A. M. Hammad, *American Chemical Society Omega*, **6**, 27737(2021), https://doi.org/10.1021/acsomega.1c02989
59. M. E. García-Pastor, P. J. Zapata, S. Castillo, D. M. Romero, F. Guillen, D. Valero and M. Serrano, *Frontier Plant Science*, **11**, (2020), https://doi.org/10.3389/fpls.2020.00668
60. A. M. Ghahfarokhi and R. Farhoosh, *Scientific Reports*, **10**, (2020), https://doi.org/10.1038/s41598-020-76620-2
61. I. Lini, S. Mlinari, L. Brklja˘ci, I. Pavlovi, A. Smolko and B. S. Sondi, *Plants*, **10(11)**, 2346(2021), https:// doi.org/10.3390/plants10112346
62. M. A. Esawi, H. O. Elansary, N. A. Shanhorey, A. M. E. Abdel-Hamid, H. M. Ali and M. S. Elshikh, *Frontier Physiology*, **8**, 1(2017), https://doi.org/10.3389/fphys.2017.00716
63. H. C. Koa, M. G. Janga, J. W. Kima, S. Baeka, N. H. Leeb and S. J. Kim, *InternationalJournal of Food Properties*, **24**, 210(2021), https://doi.org/10.1080/10942912.2021.1873362
64. J. Chen, W. Lu, H. Chen, X. Bian and G. Yang, *Biological and Pharmaceutical Bulletin*,**42**, 231(2019), https://doi.org/10.1248/bpb.b18-00661
65. S. Kundan, G. D. Bajju, D. Gupta and T. K. Roy, *Russian Journal of Inorganic Chemistry*,**64**, 1379(2019), https://doi.org/10.1134/S003602361911010X

[RJC-7019/2022]